Lesne et al. Supplemental Material

		-	A	D	E	F	G	H	I	K	L	M	N	P	Q	R	S	T	V	W	Y
VFT2	V	0.0	53	0	12	4	5	9	26	3	13	5	86	0	9	68	45	60	20	0	4
	S	0.0	19	12	11	0	33	6	9	8	20	9	177	0	10	11	72	13	2	0	10
	R	0.0	2	15	6	0	1	19	0	81	1	2	4	4	10	268	1	7	0	0	1
	W	0.0	0	0	0	0	0	1	0	0	0	0	0	0	0	0	0	0	0	421	0
	R	0.0	5	0	4	7	4	13	6	2	56	5	4	0	41	248	11	7	5	1	3
	G	0.0	48	7	4	0	132	1	3	13	1	1	36	25	8	15	78	34	13	0	3
	S	0.0	52	16	45	8	3	8	8	14	4	13	43	29	3	20	37	20	24	1	74
	D	0.0	61	14	20	3	14	10	16	9	7	3	9	72	8	8	51	33	80	0	4
	G	0.0	58	27	27	5	32	2	22	7	43	10	20	41	12	4	16	15	55	0	26
	D	0.0	39	5	11	9	7	18	42	8	20	40	3	51	21	16	23	15	94	0	0
	P	0.0	40	50	49	3	22	5	3	17	1	0	18	35	19	10	100	27	19	0	4
H19	R	0.0	17	97	22	2	77	1	24	7	25	4	19	38	24	9	22	7	23	0	4
	T	0.0	19	37	17	1	30	8	18	2	17	2	35	34	42	10	109	20	15	0	6
	W	0.0	23	20	1	23	6	2	10	2	10	2	18	8	3	8	58	122	9	22	75
	Y	0.0	1	4	2	15	6	5	1	0	8	7	1	7	3	6	23	4	0	324	5
	A	0.0	16	19	25	2	7	14	2	12	32	4	21	7	60	111	18	12	28	25	7
	Y	1.0	22	75	28	5	18	11	1	17	34	2	40	3	12	94	20	15	5	6	13
	R	4.0	6	6	6	13	0	33	30	10	22	2	34	2	3	15	5	5	30	0	196
	N	14.0	28	4	11	1	7	34	4	17	17	2	20	23	31	149	29	5	7	2	17
	E	47.0	16	7	9	1	18	10	2	22	14	0	11	19	32	118	37	36	9	4	10

Figure S1. Composition of the last periplasmic stretch in the BvgS family. The matrix represents the composition of 422 BvgS homologs. To optimize the sequence alignments, the 140 proteins devoid of the 'RWR' motif that terminates the VFT2 domain were not included in this analysis. The first column shows the sequence of BvgS, from the last residues of the VFT2 domain to the residue preceding the predicted TM segment. Note that in BvgS H19 starts after the Pro residue. The matrix shows the frequency at which each of the 20 residues is found at each BvgS sequence position. The second column indicates the gaps, i.e. the proteins that are 1, 2, 3 or 4 residues shorter than BvgS in this region according to the alignments.

	A	C	D	E	F	G	H	I	K	L	M	N	P	Q	R	S	T	V	W	Y
I	39	0	0	8	58	6	5	39	17	147	9	4	8	16	23	9	26	72	54	22
Y	30	0	1	0	69	9	3	194	6	57	13	2	2	0	6	4	12	66	39	49
L	32	0	0	3	15	21	4	84	6	113	14	0	2	28	11	11	20	36	41	121
L	30	0	0	20	13	26	5	37	21	67	8	6	16	141	18	17	26	62	40	9
I	65	1	0	0	28	67	0	145	1	81	6	0	10	4	0	20	28	97	7	2
G	59	1	0	0	51	56	0	95	4	90	12	0	6	0	0	34	13	137	3	1
L	142	5	0	0	15	72	0	99	3	113	6	1	3	0	0	22	20	57	4	0
G	118	10	0	0	37	123	0	52	0	88	10	0	4	0	0	27	22	71	0	0
L	219	10	0	0	24	30	0	35	0	68	11	0	0	0	0	47	51	67	0	0
L	84	10	0	0	30	79	0	39	0	169	8	0	4	0	0	51	19	69	0	0
S	41	3	0	0	25	22	0	49	0	279	7	0	1	0	0	13	13	109	0	0
A	33	1	0	0	41	5	0	67	0	294	13	0	1	0	0	11	21	75	0	0
L	44	2	0	0	16	37	0	67	0	297	8	0	0	0	0	14	11	63	2	1
L	47	6	0	0	17	22	0	63	0	288	13	1	0	0	0	33	16	53	3	0
F	58	7	0	0	34	29	0	67	0	189	23	0	0	0	0	41	21	86	5	2
L	88	8	0	0	29	22	5	46	0	127	4	0	0	0	0	146	22	62	3	0
S	29	4	0	0	46	34	9	68	0	264	12	0	0	0	0	18	8	59	7	4
W	103	3	0	0	35	63	3	66	0	70	5	3	0	0	2	6	17	60	91	35
I	23	1	0	0	24	30	5	48	0	27	2	18	0	1	14	12	5	22	309	21
V	32	2	0	0	26	38	3	58	0	45	3	158	0	1	10	35	11	49	39	52
Y	98	4	1	0	39	15	11	31	4	77	3	21	0	1	36	43	16	25	42	95
L	11	3	1	0	8	7	25	7	15	105	16	19	0	9	113	25	16	9	35	138

Figure S2. Composition of the putative transmembrane stretch in the BvgS family. The first column shows the sequence of BvgS, and the other columns indicate the frequencies of each of the 20 residues at each sequence position.

	-	A	C	D	E	F	G	H	I	K	L	M	N	P	Q	R	S	T	V	W	Y
-	375	0	0	0	0	0	0	1	0	0	0	0	2	0	0	0	0	0	0	0	0
-	371	0	0	0	0	0	0	0	0	0	1	0	0	0	0	2	0	4	0	0	0
-	88	4	3	0	0	5	6	15	3	1	7	8	1	0	7	67	19	2	1	17	124
-	10	1	0	0	0	1	0	0	8	0	272	70	0	0	5	4	0	7	0	0	0
R	4	10	0	1	0	0	2	11	0	38	16	2	14	0	11	253	5	4	3	2	2
R	4	9	1	0	0	1	13	8	10	26	13	3	5	0	9	237	15	4	16	3	1
Q	4	9	0	0	37	0	0	8	1	9	54	1	1	0	243	6	4	0	1	0	0
I	4	10	0	0	0	2	0	2	244	0	4	15	1	0	1	0	0	2	81	0	12
R	2	13	0	3	1	5	9	13	6	78	11	0	11	0	24	178	16	5	3	0	0
Q	0	27	0	1	19	0	1	10	3	68	18	5	3	0	136	66	8	5	5	1	2
R	0	1	1	0	9	0	1	0	0	11	2	0	0	0	3	341	2	6	1	0	0
K	0	22	0	10	43	1	0	4	6	75	47	0	2	0	75	63	7	9	14	0	0
R	0	75	3	4	24	2	0	6	9	51	33	10	6	0	61	63	6	9	15	0	1
A	0	299	0	1	6	0	0	0	10	3	7	2	1	0	1	0	24	7	17	0	0
E	0	1	0	2	279	0	1	0	0	14	0	1	2	0	61	15	0	1	1	0	0
R	0	18	0	1	13	0	11	12	5	27	20	2	8	0	52	180	12	8	7	0	2
A	0	220	0	9	29	0	4	1	1	8	12	7	8	0	36	30	4	8	1	0	0
L	0	0	0	0	2	1	0	0	2	0	370	2	0	0	0	0	0	0	1	0	0
N	0	4	0	7	28	0	22	5	2	14	8	0	144	0	41	6	89	6	1	0	1
D	0	19	0	244	44	0	4	0	0	1	3	0	26	0	10	0	4	10	3	0	10
Q	0	2	0	0	13	0	0	7	0	5	4	0	0	0	324	19	3	0	1	0	0
L	0	7	0	0	1	37	0	0	10	0	264	26	2	0	1	1	1	0	21	1	6
E	0	93	0	2	118	0	6	1	5	23	4	1	8	0	29	37	25	14	11	0	1
F	0	0	0	1	0	334	0	0	0	1	26	0	0	0	6	0	1	0	2	0	7
M	0	0	0	1	2	0	0	2	28	41	20	186	6	0	38	25	3	2	16	8	0
R	0	5	0	12	59	10	21	14	0	16	0	0	7	0	42	163	17	8	4	0	0
V	0	145	0	11	11	0	0	2	3	1	3	0	8	0	4	1	47	79	63	0	0
L	0	0	0	0	0	2	0	0	7	0	334	23	0	0	0	0	0	0	12	0	0
I	0	1	0	1	0	22	7	0	121	0	98	0	3	0	0	0	12	23	89	0	1
D	0	3	0	192	15	0	1	2	0	1	0	0	158	0	1	0	3	2	0	0	0
G	0	18	10	4	8	1	264	0	0	0	0	0	4	0	0	0	62	6	1	0	0
T	0	1	0	0	0	0	0	0	81	0	45	49	1	0	1	0	6	190	3	0	1

Figure S3. Composition of the cytoplasmic portion of Linker 1 in the BvgS family. The matrix represents the composition of 378 BvgS homologs. To optimize the alignments, the 127 proteins devoid of a PxP motif at the entry of the PAS core domain were not included in the analysis. The first column shows the sequence of BvgS, from the end of the predicted transmembrane segment to the residue immediately preceding the first Pro of the PxP motif. This first column indicates also the proteins that are one to four residues longer than BvgS while the second column indicates those that are one to five residues shorter than BvgS, according to our alignment.

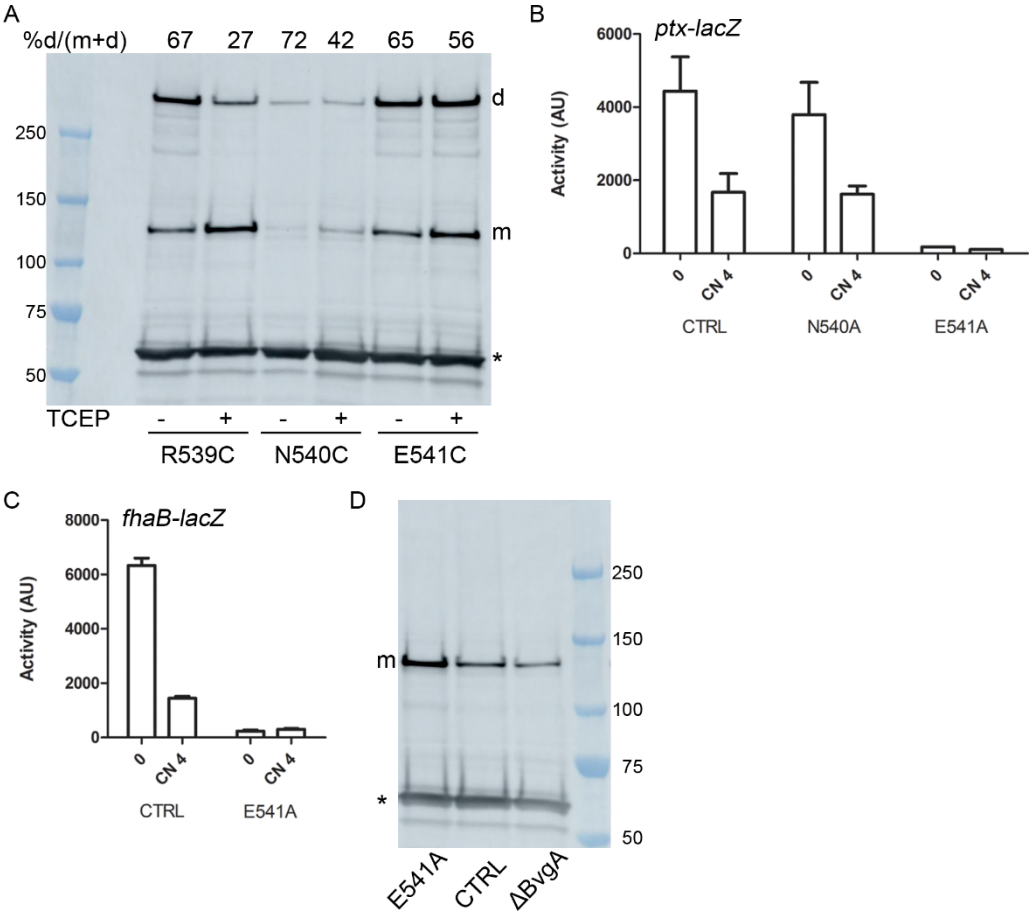

Figure S4. Characterization of BvgS^{fl} variants with substitutions in H19. (A). Immunodetection of BvgS in monomeric (m) or dimeric (d) forms from membrane extracts of *B. pertussis* producing the indicated BvgS^{fl} variants, at the basal state or after addition of 10 mM TCEP six hours before harvesting the bacteria. (B) and (C). The *ptx-lacZ* (B) and *fhaB-lacZ* (C) reporters were used to determine the activities of the BvgS^{fl} variants in *B. pertussis* grown in normal conditions or in the presence of 4 mM chloronicotinate. All variants harbor the $C_{607}A$ and $C_{881}S$ substitutions as in the control (CTRL), which corresponds to the strain producing BvgS^{fl}. The means and standard errors of the mean are indicated. (D). Immunodetection of BvgS from *B. pertussis* membrane extracts. The avirulent, *ΔbvgA* strain is used as a control to show the abundance of BvgS in an avirulent strain. The loading control is an unidentified *B. pertussis* protein fortuitously recognized by the antibodies (indicated with an asterisk).

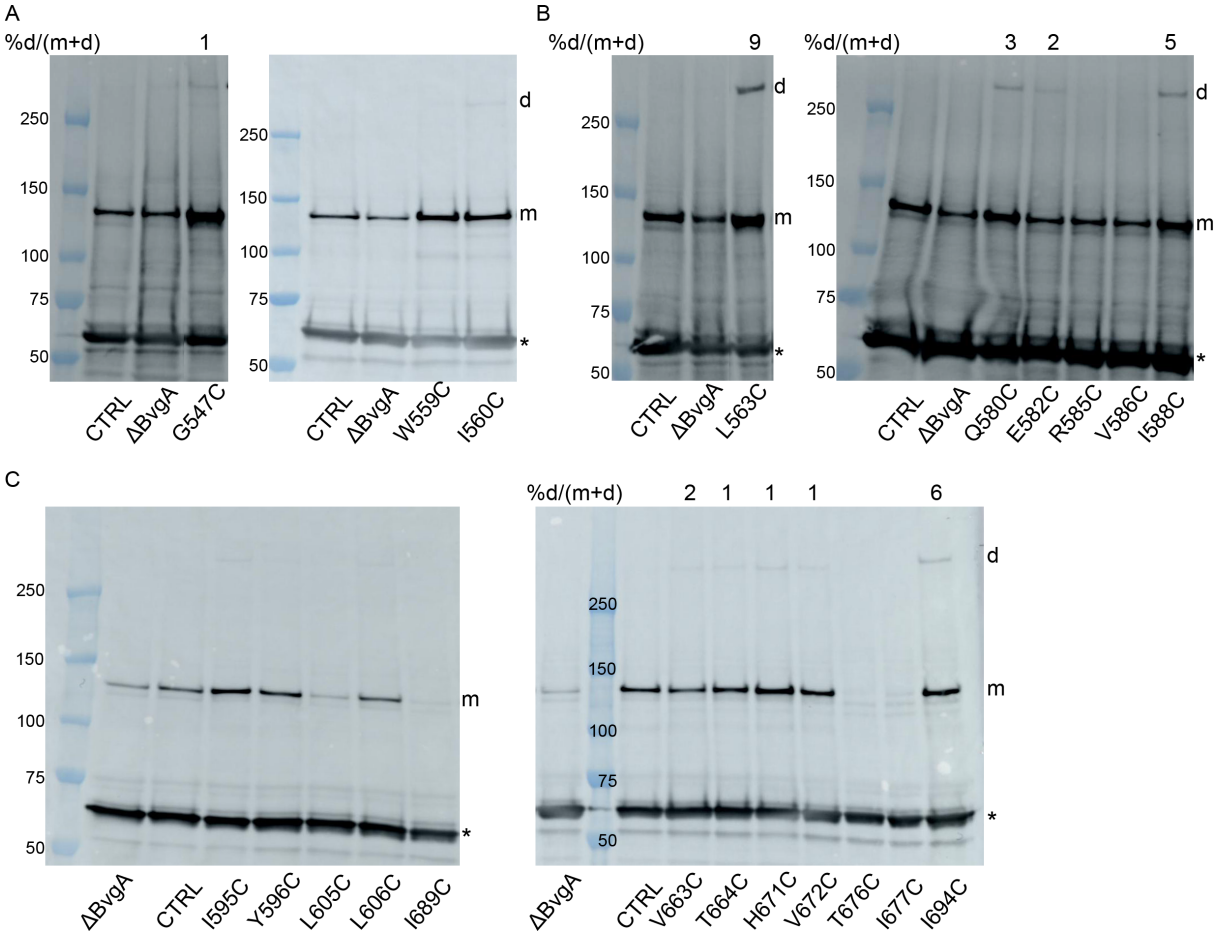

Figure S5. Immunoblot analyses of selected BvgS^{fl} variants with Cys substitutions. BvgS^{fl} variants for which the reporter fusions indicated a major activity defect were subjected to immunoblotting from *B. pertussis* membrane extracts. The levels of production of the variant proteins and the extent of spontaneous S-S bond formation were thus determined. The Cys substitutions are in the transmembrane segment (A), in the cytoplasmic linker 1 (B) or in the PAS domain (C). Spontaneous formation of S-S bonds between monomers (m) results in the presence of dimers (d), whose proportions are indicated at the top of each lane. All variants harbor the $C_{607}A$ and $C_{881}S$ substitutions as in the control (CTRL), which corresponds to the strain producing BvgS^{fl}. The loading control is indicated with an asterisk.

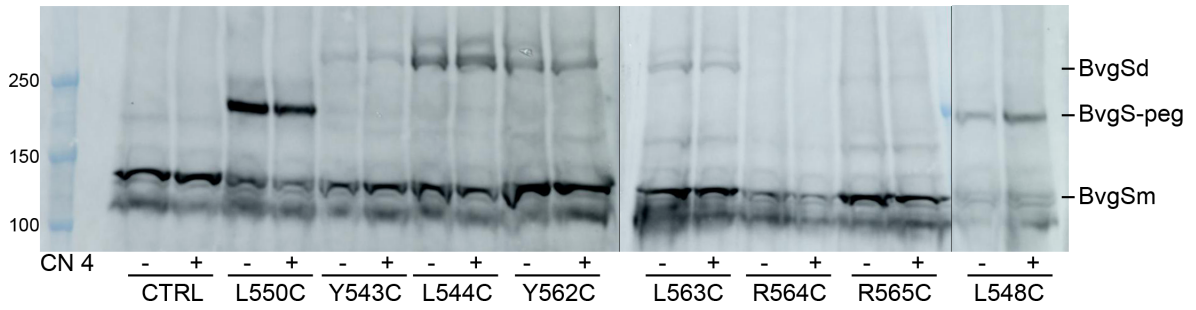

Figure S6. Cys accessibility in the hydrophobic segment. Cysteine accessibility was determined under basal conditions or after addition of 4 mM chloronicotinate for the indicated BvgS^{fl} variants. Monomeric and dimeric BvgS, or BvgS fixed with peg-maleimide are indicated by BvgSm, BvgSd and BvgS-peg, respectively. All variants harbor the $C_{607}A$ and $C_{881}S$ substitutions, as in the control (CTRL), which corresponds to the strain producing BvgS^{fl}.

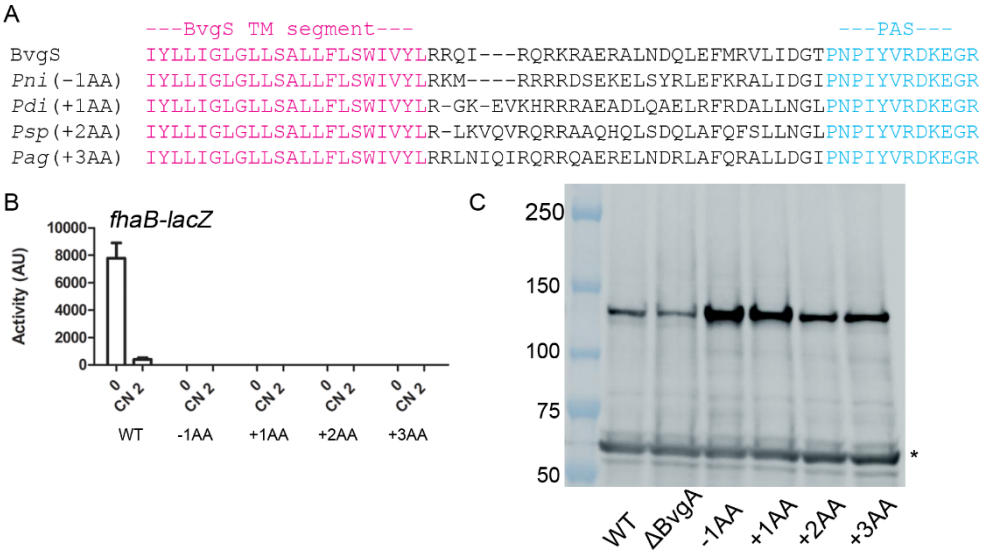

Figure S7. Influence of the length of the cytoplasmic portion of Linker 1 on BvgS activity. (A). Sequences of chimera harboring the cytoplasmic portion of Linker 1 from homologs, inserted between the transmembrane (pink letters) and PAS (blue letters) domains of BvgS. The species from which the sequences originate are indicated as follows: *Pni, Pseudomonas nitroreducens* (GI 516088738), *Pdi, Pantoea dispersa* (GI 545152798), *Psp, Pseudomonas sp. CF161* (GI 520812285) and *Pag*, *Pseudomonas agarici* (GI 984943149). (B). The activities of the BvgS^{fl} variants were determined using the *fha-lacZ* reporter under basal conditions (0) or after perception of 4 mM chloronicotinate (CN 4). C. Immunoblot analyses of BvgS variants in membranes extracts of *B. pertussis*. The loading control is indicated with an asterisk.

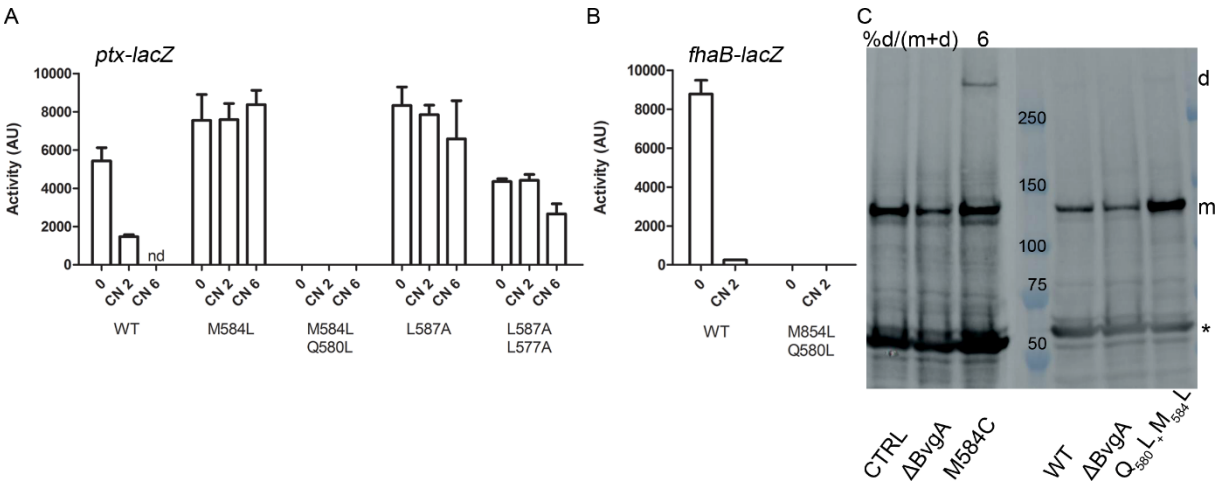

Figure S8. Characterization of selected BvgS variants. (A) and (B). The *ptx-lacZ* (A) or *fhaB-lacZ* (B) reporter systems were used to determine the activities of the BvgS variants in *B. pertussis* grown under basal conditions or after perception of millimolar concentrations of chloronicotinate. The natural Cys residues were present as in the wt strain. The means and standard errors of the mean are indicated. (C). Immunoblot analyses of BvgS variants in membranes extracts of *B. pertussis*. The proportions of dimers (d) due to spontaneous S-S bond formation between monomers (m) are indicated at the top of each lane. In the left panel, the $BvgS^{fl}_{M584C}$ variant harbor the $C_{607}A$ and $C_{881}S$ substitutions as in the $BvgS^{fl}$ control (CTRL). The loading control is indicated with an asterisk.